Construction and Building Materials xxx (xxxx) xxx

Contents lists available at ScienceDirect

Construction and Building Materials

journal homepage: www.elsevier.com/locate/conbuildmat

Experimental characterization of the axial behavior of traditional masonry wall metal tie connections in cavity walls

Onur Arslan [a,b,*], Francesco Messali [c], Eleni Smyrou [d], İhsan E. Bal [e], Jan G. Rots [f]

[a] Faculty of Civil Engineering and Geosciences, Delft University of Technology, Delft, the Netherlands
[b] Research Centre for Built Environment NoorderRuimte, Hanze University of Applied Sciences, Groningen, the Netherlands
[c] Faculty of Civil Engineering and Geosciences, Delft University of Technology, Delft, the Netherlands
[d] Research Centre for Built Environment NoorderRuimte, Hanze University of Applied Sciences, Groningen, the Netherlands
[e] Research Centre for Built Environment NoorderRuimte, Hanze University of Applied Sciences, Groningen, the Netherlands
[f] Faculty of Civil Engineering and Geosciences, Delft University of Technology, Delft, the Netherlands

HIGHLIGHTS

- Assessing the seismic response of the wall tie connections in cavity walls.
- Results obtained in terms of average force-displacement curves/failure mechanisms.
- Additional characterization tests on the materials performed.
- Embedment length and geometry of tie influences the capacity of the connection.
- Precompression level and loading rate does not have a significant influence.

ARTICLE INFO

Article history:
Received 16 October 2019
Received in revised form 23 September 2020
Accepted 25 September 2020
Available online xxxx

Keywords:
Unreinforced masonry
Cavity walls
Wall ties
Cyclic tests

ABSTRACT

In recent years, the number of human-induced earthquakes in Groningen, a large gas field in the north of the Netherlands, has increased. The majority of the buildings are built by using unreinforced masonry (URM), most of which consists of cavity (i.e. two-leaf) walls, and were not designed to withstand earthquakes. Efforts to define, test and standardize the metal ties, which do play an important role, are valuable also from the wider construction industry point of view. The presented study exhibits findings on the behavior of the metal tie connections between the masonry leaves often used in Dutch construction practice, but also elsewhere around the world. An experimental campaign has been carried out at Delft University of Technology to provide a complete characterization of the axial behavior of traditional connections in cavity walls. A large number of variations was considered in this research: two embedment lengths, four pre-compression levels, two different tie geometries, and five different testing protocols, including monotonic and cyclic loading. The experimental results showed that the capacity of the connection was strongly influenced by the embedment length and the geometry of the tie, whereas the applied pre-compression and the loading rate did not have a significant influence.

1. Introduction

The number of human induced earthquakes in the province of Groningen, located in the northern part of the Netherlands, has considerably increased in the last decade. Most of the existing buildings in that area are composed of unreinforced masonry (URM) and were not designed to withstand earthquakes, since the area had never been affected by tectonic earthquakes. Hence, the assessment of URM structures in the Groningen province has become of high relevance in earthquake engineering community. The majority of the buildings in the region are characterized by slender walls, large openings and cavity walls (i.e. double-leaf walls with an air gap in between). Specifically, buildings with double-leaf cavity walls constitute a large portion of the building stock in the Groningen gas field.

A cavity wall consists of two separate parallel walls, with an inner load-bearing masonry wall and an outer veneer mostly with aesthetic and insulating functions. In case of the Dutch construction practice, calcium silicate brick masonry is used for the inner

* Corresponding author.
E-mail addresses: o.arslan@tudelft.nl, o.arslan@pl.hanze.nl (O. Arslan), F. Messali@tudelft.nl (F. Messali), e.smyrou@pl.hanze.nl (E. Smyrou), i.e.bal@pl.hanze.nl (İ.E. Bal), J.G.Rots@tudelft.nl (J.G. Rots).

https://doi.org/10.1016/j.conbuildmat.2020.121141
0950-0618/

leaves, whereas solid or perforated clay brick masonry is used for the outside veneer leaf. The inner and outer leaves are interconnected by means of metal ties, as prescribed in NEN-EN 845-1 [1]. This study aims at investigating the structural response of wall ties commonly used in the traditional Dutch construction practice to connect the two masonry leaves of cavity walls, a practice used also in other parts of the world.

An extensive multiscale testing program was performed at TU Delft in 2015, the results of which are presented in Messali [2]. Part of the research focused on terraced houses built in the Netherlands during the period 1960–1980 [3,4] and characterized by the use of cavity walls. The double-leaf masonry construction also exists in other regions of the world, such as Australia, New Zealand, and North America, as well as in various parts of northern Europe. In the framework of the same multiscale testing campaign, an integrated testing program was carried out at EUCENTRE laboratories in Pavia in 2015, where, among others [5], two full-scale shake table tests were conducted on terraced houses [6,7]. Furthermore, recent shake table experiments [8,9] on single-leaf and double-leaf cavity walls clearly underline the dominance of out-of-plane failure mode in these slender URM walls.

The out-of-plane behavior is a common failure mechanism of slender masonry walls during an earthquake, which often stems from poor wall-to-wall, wall-to-floor or wall-to-roof connections that provide insufficient restraint to overturning. Cavity walls are particularly vulnerable to out-of-plane mechanisms due to the slender geometry of the two leaves, and, in fact, the out-of-plane behavior of cavity walls represents a major concern during a strong shock [6,7,10]. In a study where full-scale brick veneer wall panel specimens are tested [11], it was found that out-of-plane wall damage occurred when the veneer moved away from the interior wood backup, placing a high demand on the tensile force and displacement capacities of the ties, underlining the prominent role of the ties in the composite response of the two leaves. Giaretton et al. [12] showed that, when a sufficient number of connections are used, the out-of-plane failure of cavity walls can be prevented. According to BSI PD 6697:2010 [13] a minimum number of wall ties per unit can be calculated, which is not less than 2.5 ties per square meter and should be used for walls with both leaves having size of 90 mm or thicker, whereas the spacing, embedment length in the mortar and inadequate number of ties will influence the overall capacity of the cavity wall.

In the study by Walsh et al. [10], in-situ tests were carried out on full scale masonry cavity walls for both existing and retrofitted metal ties, concluding that the retrofitting of cavity walls with adequate spacing, as well as adequate compressive and shear stiffness, can greatly improve the OOP capacity of URM walls. Also few laboratory tests were conducted for investigating the behavior of URM cavity walls on both existing ties [8,9,14] and on retrofitted ties [15,16], where various failures in ties have occurred.

Choi and LaFave [17] and Reneckis and LaFave [18] performed experiments at component level on brick-tie-wood, representing current U.S. construction practice. The monotonic tests (tension, compression, and shear) and the cyclic tests were carried out to capture the local performance of overall wall systems in order to assess the influence of tie thickness, initial offset displacement, attaching method of ties to wood studs, type of loading, eccentricity and embedment length. They found that the workmanship of brick veneer, particularly with respect to the installation of the ties, plays an important role on the overall wall system performance.

An experimental investigation had been performed on different brick-tie-brick assemblages on the connections in cavity walls based on construction practices from Portugal and other South European countries [19], evaluating the response at component level under cyclic loading in terms of stiffness, strength, dissipation of energy and failure modes. They concluded that the main role of the cavity wall ties on masonry outer leaves is the transfer of out-of-plane lateral loads from the outer leaves to inner leaves through the connection between both elements. For this reason, Martins et al. [19] state that the ties should have an adequate resistance and stiffness both in tension and compression. They also concluded that the tie shape and geometry were the most important factors influencing the strength of the tie connections.

An experimental campaign on cavity wall ties was carried out at TU Delft to characterize of the behavior of the connections in terms of resistance, envelope curve and dissipated energy [20]. The specimens were typical wall ties used in Dutch terraced houses, embedded either in calcium silicate or in perforated clay brick couplets. Different loading conditions (axial and shear, monotonic and cyclic loading) and different confining compressive loads on the couplets were considered. It was found that the wall ties tested were able to connect the two leaves for relatively small seismic out-of-plane displacement demands but might fail in larger wall out-of-plane displacements, even before the wall reaches collapse capacity.

This paper presents the outcome of experiments carried out at the Macrolab/Stevin laboratory of TU Delft. The experiments aim to provide a complete characterization of the axial cyclic behavior of cavity wall ties. This research can also provide a better understanding of the behavior of the tested metal wall ties for the industry to find suitable methods for developing their products and improve the seismic response of existing URM structures. Section 2 of the paper describes the specimen geometry, the test-setup, the adopted testing protocol and the tests carried out to characterize the used materials. It describes also the characteristics of the groups of specimens tested, obtained by a combination of different materials, geometry and loading protocols. Section 3 presents and discusses the test results, with special attention on the developed failure mechanism and on the definition of average force–displacement curves for each group of tests performed.

2. Experiments conducted

2.1. Description of the specimens

The experiments presented here aim to characterize the axial cyclic behavior of metal cavity wall ties. Each specimen consisted of two bricks connected by means of mortar (couplets) and included an embedded metal wall tie that was designed to be representative of a portion of as-built URM cavity walls. 202 couplets were tested in total, consisting of two types of masonry units: solid calcium silicate (CS) and perforated clay brick masonry (CB). Ties were placed inside the mortar bed-joint, as happens in real applications (Figs. 1 and 2). The flow of the mortar was determined in agreement with NEN-EN 1015–3 [21]. During the construction phase, no free movement of the ties was allowed inside fresh mortar, and the specimens were built in agreement with NEN-EN 845–1 + A1 [1]. In practice, the zigzag-end is embedded in the CB masonry, while the L hook-end is embedded in the inner CS walls, as shown in Fig. 1.

L-shaped ties with a diameter of 3.6 mm and a total length of 200 mm were embedded between two bricks in the mortar joint. The embedment length was different at each end of the tie: the zigzag-end was embedded for a length of 50 mm, whereas the hooked-ends were embedded for two different lengths of the straight portions, 70 mm and 50 mm, representing possible variations in practice. For a number of specimens, the tie was bent 15° from the axis perpendicular to the vertical, representing imperfect applications often observed in practice. From the previous campaign [20], the bent tie was embedded in the CS masonry because the test results highlighted that the tie connections in the inner

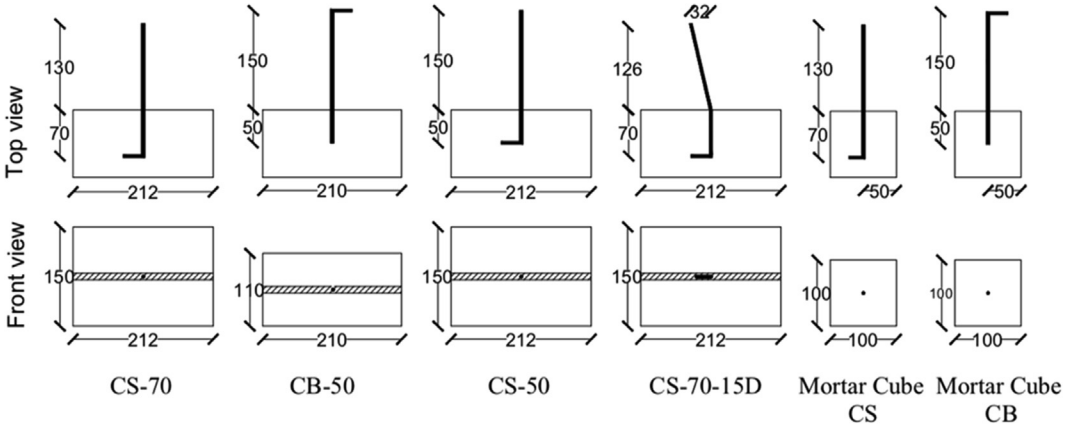

Fig. 1. Geometry of tie specimens.

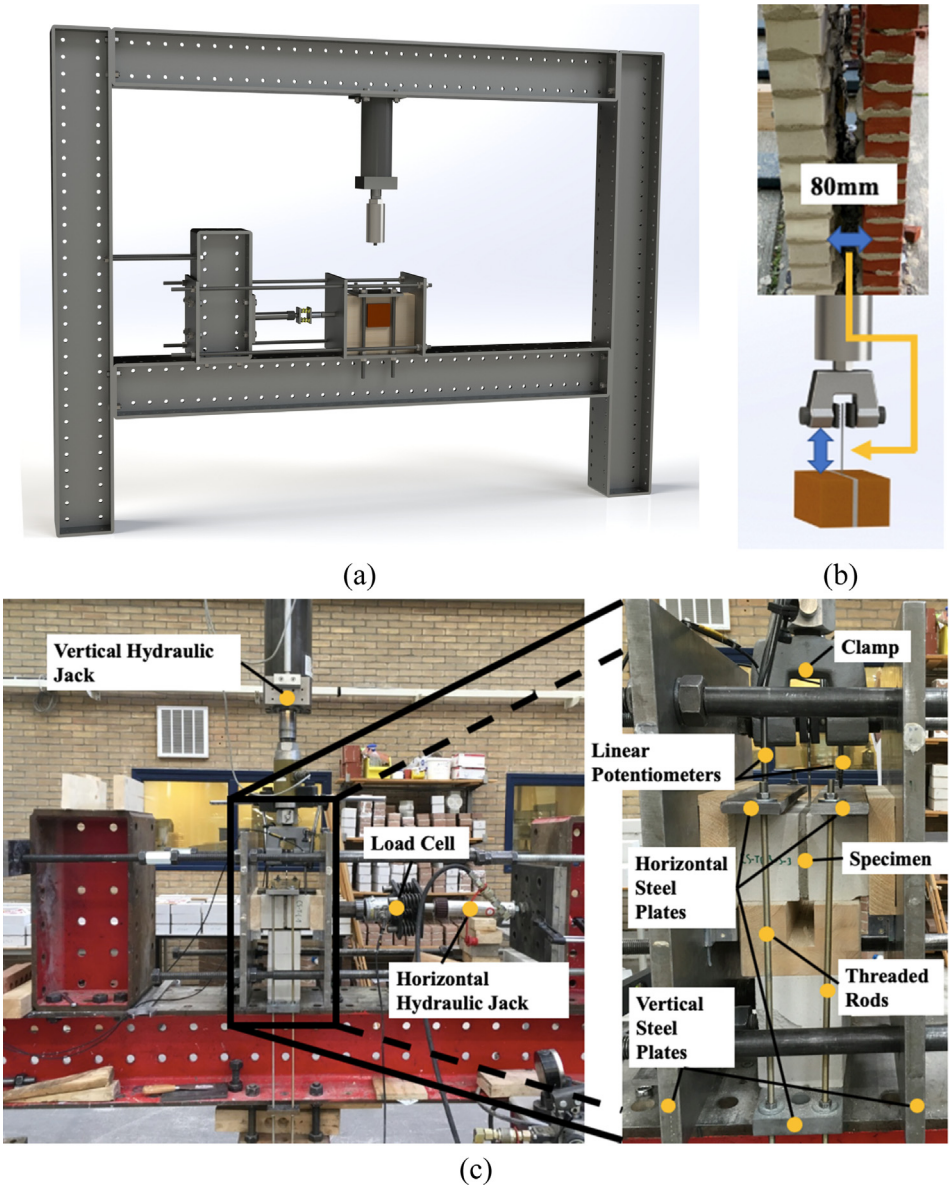

Fig. 2. Testing setup: General setup (Skroumpelou et al. 2018) (a); Axial setup (b); Test setup (c).

leaf play a critical role in overall wall performance. In addition to the masonry couplets, 32 mortar cube samples were constructed to investigate the embedment of the tie in the mortar alone. A number of specimens tested in the current experiment campaign were chosen for establishing force–displacement curve accurately and indicating the variability of the material. Specimens which reached their full capacity are presented in this paper. As in practice in the Dutch construction, mortar used for CS and CB layers is different [2,8]. In mortar cube tests with ties, both mortar types were tested. For each of these specimens, the tie was embedded into the mortar cube with an anchoring length of 70 mm for mortar used with CS, or 50 mm for mortar used in CB bricks. To provide a complete characterization of the connection typology, six types of specimens were eventually tested as shown in Table 1 and Fig. 1:

- CS-70: the hooked part of the tie is embedded in a CS couplet, with 70 mm anchoring length;
- CS-70-15D: the hooked part of the tie is embedded in a CS couplet, with 70 mm, the zigzag-end of the tie is bent 15°;
- CS-50: the hooked part of the tie is embedded in a CS couplet with a reduced embedment length of 50 mm;
- CB-50: the zigzag-end part of the tie is embedded in a CB couplet, with an anchoring length of 50 mm;
- Mortar Cubes of CS Mortar: the hooked part of the tie is embedded in a mortar cube made of the same mortar used for the CS couplets, with an anchoring length of 70 mm;
- Mortar Cubes of CB Mortar: the zigzag-end part of the tie is embedded in a mortar cube made of the same mortar used for the CB couplets, with an anchoring length of 50 mm.

2.2. Test setup and the loading protocol

The test setup was assembled based on the recommendations reported in NEN-EN 846–5 [22] and is shown in Fig. 2. The testing machine was connected to a contrast steel frame, integrated with a data acquisition system (Fig. 2a). The specimen was placed in the test machine so that the tie lay aligned vertically along the centerline axis of the test machine, and the tie was clamped to have a free distance from the couplet equal to 80 mm (Fig. 2b), a gap representative of the Dutch construction practice. An image of the setup with the names of the different components is shown in Fig. 2c.

During the test, a horizontal compressive force was applied to the couplet and maintained constant by a manually operated hydraulic jack. Two lateral steel plates ensured the diffusion of the compressive load on the entire lateral surfaces of the couplets. Different levels of pre-compression were applied to the specimens: 0 MPa, 0.1 MPa, 0.3 MPa, and 0.6 MPa. The applied precompression levels were considered to be representative of a cavity wall at different level of a typical URM residential building regardless of the boundary conditions. The axial load applied vertically to the wall tie using a displacement-controlled apparatus equipped with a jack. The machine was provided with a clamp for gripping

Table 1
Specimens tested for each loading protocol.

Specimen Type	Loading Protocol	Lateral Precompression (MPa)	Embedment Length (mm)	Bending (deg)	Number of specimens
CS-70	MT	0.1	70	0	11
	MT	0.3	70	0	10
	MT	0	70	0	3
	MT	0.6	70	0	3
	MT-HS	0.1	70	0	6
	MC	0.1	70	0	12
	MC	0.3	70	0	9
	MC	0	70	0	1
	MC	0.6	70	0	1
	MC-HS	0.1	70	0	3
	Cyclic	0.1	70	0	9
	Cyclic	0.3	70	0	11
CS-70-15D	MT	0.1	70	15	6
	MC	0.1	70	15	6
	Cyclic	0.1	70	15	8
	Cyclic	0.3	70	15	8
CS-50	MT	0.1	50	0	3
	MC	0.1	50	0	2
	Cyclic	0.1	50	0	9
CB-50	MT	0.1	50	0	12
	MT	0.3	50	0	11
	MT	0	50	0	3
	MT	0.6	50	0	3
	MT-HS	0.1	50	0	6
	MC	0.1	50	0	10
	MC	0.3	50	0	10
	MC	0	50	0	1
	MC	0.6	50	0	1
	MC-HS	0.1	50	0	3
	Cyclic	0.1	50	0	10
	Cyclic	0.3	50	0	11
Mortar Cubes for CS	MT	0	70	0	3
	MC	0	70	0	3
	Cyclic	0	70	0	10
Mortar Cubes for CB	MT	0	50	0	3
	MC	0	50	0	3
	Cyclic	0	50	0	10

Note: MT = Monotonic Tensile; MT-HS = Monotonic Tensile High Speed; MC = Monotonic Compressive; MC-HS = Monotonic Compressive High Speed.

efficiently the free-end of the tie. The vertical displacements of the bricks of the couplets were prevented by two horizontal steel plates connected by steel threaded rods. Two linear potentiometers were installed symmetrically on the two opposite sides of the clamp, pointing against the steel plate on top of the couplet. Their measuring range was 10 mm (Fig. 2).

The specimens were subjected to two different loading regimes which are quasi-static monotonic and cyclic loading. Two loading speeds were conducted for the monotonic tests: (1) quasi-static loading rate which is considered to be conservative and (2) high-speed rate investigating the effect of speed rates closer to those that occur during earthquakes. The nominal displacement corresponding at the peak force was determined by the monotonic tests. From monotonic tests, it was possible to define the cyclic group amplitude with the increments of three cycles each time in the first phase, and then is followed by two degradation cycles that were repeated at higher amplitudes in the second phase with the purpose of capturing the cyclic degradation on the tie-mortar bond. Five different loading schemes were applied:

- MT (Monotonic Tensile): the pull-out displacements (introducing tensile loading in the connection) are increased monotonically with a rate of 0.1 mm/s up to failure.
- MT-HS (Monotonic Tensile High Speed): the pull-out displacements (introducing tensile loading in the connection) are increased monotonically with a higher rate of 1 mm/s up to failure.
- MC (Monotonic Compressive): the displacements of the clamp towards the couplet (introducing compressive loading in the connection) are increased monotonically with a rate of 0.1 mm/s up to failure.
- MC-HS (Monotonic Compressive High Speed): the displacements of the clamp towards the couplet (introducing compressive loading in the connection) are increased monotonically with a higher rate of 1 mm/s up to failure.
- C (Cyclic): the displacements imposed to the clamp are cyclically varied to apply both tensile and compressive loads to the connection. The loading history for this test is divided into two phases. In phase 1, three groups of three cycles of amplitude equal to 0.1 mm, 0.25 mm and 0.5 mm, are performed. In phase 2 each cycle is composed by two runs of increased amplitude with respect to the previous cycle and two runs of reduced displacement, calculated as 40% of the displacements of the two previous runs (Fig. 3). The loading rate is chosen to maintain a constant duration of every cycle until reaching 1 mm/s. Afterwards it is kept constant.

2.3. Mechanical characterization of the materials

A series of companion tests were performed to characterize the mechanical properties of the materials used in the testing campaign. The flexural and compressive strength of the mortar, the tensile and compressive capacity of the tie, and the bond strength between masonry unit and mortar were investigated.

The tension properties of the tie were defined in terms of average values of elastic modulus (E_3), yield strength (f_y), yield strain (ε_y), tensile strength (f_t), strain at tensile strength (ε_t) and elongation at rupture (ε_r) according to ASTM E8/E8M-16a [23]. The Young's modulus was derived as the chord elastic modulus evaluated between 1/10 and 1/3 of the tensile strength. The yielding of the tie occurred at a stress level approximately 1/3 of the tensile strength. The behavior of the connection under compressive loading was interpreted in terms of Euler's buckling. The compression properties of the tie were defined in terms of strength at Euler's critical load (f_{ct}) and strain at critical load (ε_{ct}) according to ASTM E9-19 [24]. Additionally, the column effective length factor (K) computed via the experimental results, is also reported. A summary of the connection mechanical properties resulting from material characterization tests is reported in Table 2.

The mechanical characterization of the mortars both for CS and CB were defined in terms of mean compressive strength (f_b) and flexural strength of mortar (f_x) in agreement with NEN-EN 1015–11 [25], and bond between the mortar (f_w) and the units. This latter parameter was investigated by means of bond-wrench tests, performed in agreement with NEN-EN 1052–5 [26]. These tests were carried out on the couplets after the testing when the bond between the mortar and the brick was not damaged. In total 27 CS couplets and 17 CB couplets were tested for material characterization. The mean bond strength was equal to 0.34 MPa (St. Dev. of 0.09 MPa) and to 0.52 MPa (St. Dev. of 0.14 MPa) for the CS and CB specimens, respectively. A stronger bond was obtained for the CB masonry compared to CS brick masonry, possibly due to the differences in the mortar used. Table 3 lists the mortar mechanical properties resulting from material characterization tests.

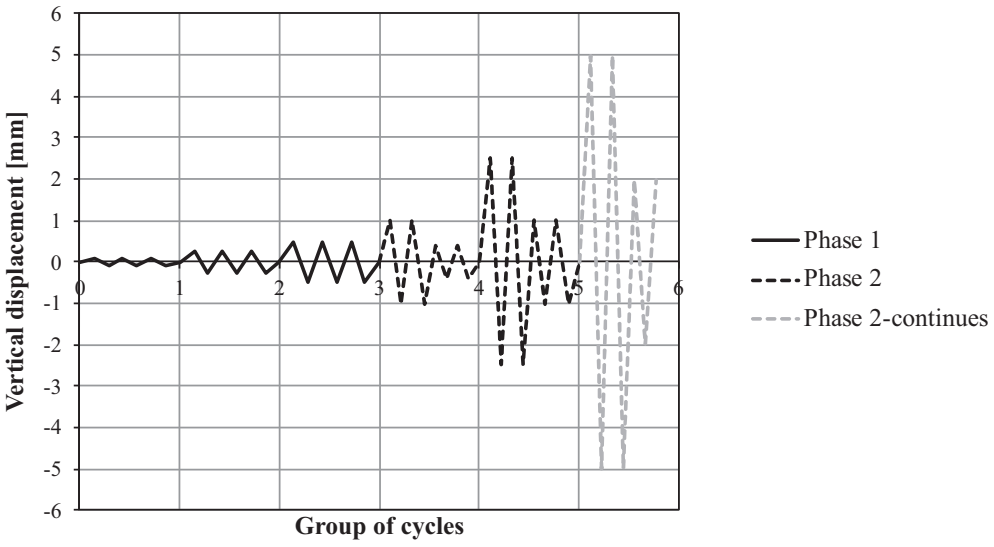

Fig. 3. Cyclic protocol.

Table 2
Summary of material characterization tests of cavity wall tie.

Loading Protocol	Material property	Symbol	UM	Tie	
				Average	**C.o.V.**
Tensile loading	Elastic modulus of tie evaluated between 1/10 and 1/3 of the maximum tensile stress	E_3	MPa	32,920	0.03
	Tie yield strength	f_y	MPa	135	0.01
	Tie yield strain	ε_y	–	0.0045	0.04
	Tie tensile strength	f_t	MPa	411	0.01
	Tie strain at tensile strength	ε_t	–	0.13	0.08
	Tie elongation at rupture	ε_r	–	0.14	0.07
Compressive loading	Tie strength at Euler's critical load	f_{ct}	MPa	198	0.05
	Tie strain at critical load	ε_{ct}	–	0.011	0.18
	The column effective length factor	K	–	0.45	–

Table 3
Mortar mechanical properties.

Material property	Symbol	UM	CS		CB	
			Average	**C.o.V.**	**Average**	**C.o.V.**
Compressive strength of mortar	f_b	MPa	5.65	0.15	6.47	0.11
Flexural strength of mortar	f_x	MPa	2.43	0.14	2.29	0.24
Flexural bond strength	f_w	MPa	0.34	0.26	0.52	0.27

3. Experimental results

This section presents the results obtained in terms of failure mechanism, average force–displacement curve, peak force, and displacement at the peak force and at failure, identified as the point of reduction by 20% of the peak force as conventionally assumed in several studies available in the literature (among other [27–29]). The specimens after reaching a 20% reduction of their peak force continued to their collapse state to observe full capacity on the connections. The tensile and compressive force–displacement curves obtained for the monotonic protocols are shown together in the same diagram for the sake of simplicity. The envelope curve regarding the cyclic loading was derived according to the recommendations provided in ASTM E2126-19 [30]. Table 4 lists the mean peak force/displacement, along with the standard deviation, and reduction by 20% of peak force. Please note that, due to the space limitations, not all curves are presented in this paper. The force–deformation response of all the experiments conducted are accessible in an open source data storage [31].

When the specimens were subjected to monotonic tensile loading, the couplets exhibited either of the following two failure mechanisms:

- Sliding failure (Type A): the tie slides along the tie-mortar interface (Fig. 4a);
- Tie failure (Type B): the tie yielding is followed by fracture of the tie (Fig. 4b).

The sliding failure mechanism, which was governed by the straightening of the tie and crushing of the surrounding mortar,

Table 4
Mean results of the axial tests (standard deviations between brackets).

Specimen type	Loading protocol	Pre-C Level (MPa)	Axial strength		Displacement at peak		Displacement at failure	
			Tensile (kN)	Comp (kN)	Tensile (mm)	Comp (mm)	Tensile (mm)	Comp (mm)
CS-70	MT, MC	0.1	2.28 (0.22)	−1.72 (0.25)	11.27 (1.98)	−3.25 (0.50)	17.1 (1.86)	−3.75 (0.55)
		0.3	2.33 (0.23)	−1.84 (0.16)	10.38 (1.49)	−3.05 (0.56)	17.9 (4.08)	−3.64 (0.78)
		0	2.54 (0.08)	−1.83	9.72 (2.81)	−3.44	11.6 (4.64)	−2.03
		0.6	2.60 (0.23)	−1.65	12.33 (0.11)	−2.85	18.1 (1.25)	−1.30
	MT-HS, MC-HS	0.1	2.30 (0.12)	−1.83 (0.19)	9.48 (0.98)	−2.90 (0.72)	16.1 (0.84)	−3.55 (0.83)
	Cyclic	0.1	1.76 (0.15)	−1.66 (0.22)	6.70 (2.28)	−2.85 (0.83)	10.6 (2.36)	−3.70 (0.75)
		0.3	1.97 (0.43)	−1.78 (0.11)	7.03 (2.88)	−2.72 (0.58)	11.0 (3.33)	−3.36 (0.31)
CS-70-15D	MT, MC	0.1	2.51 (0.13)	−1.35 (0.06)	13.07 (1.20)	−4.48 (0.82)	19.23 (3.87)	−5.04 (0.76)
	Cyclic	0.1	2.07 (0.18)	−1.45 (0.10)	9.74 (0.10)	−3.82 (0.65)	14.5 (1.27)	−4.49 (0.31)
		0.3	2.07 (0.28)	−1.44 (0.11)	9.61 (0.35)	−4.12 (0.83)	14.8 (1.54)	−4.66 (0.55)
CS-50	MT, MC	0.1	1.87 (0.14)	−1.80 (0.23)	8.25 (0.60)	−2.52 (0.13)	14.4 (0.81)	−2.92 (0.04)
	Cyclic	0.1	1.63 (0.12)	−1.96 (0.22)	4.58 (0.80)	−3.38 (1.77)	10.6 (1.19)	−4.54 (2.37)
CB-50	MT, MC	0.1	3.59 (0.56)	−1.85 (0.18)	7.16 (3.15)	−2.12 (0.31)	8.60 (3.48)	−2.45 (0.36)
		0.3	3.65 (0.35)	−1.82 (0.15)	7.90 (1.64)	−2.15 (0.22)	10.3 (2.68)	−2.51 (0.31)
		0	3.09 (0.40)	−1.94	4.27 (1.84)	−2.22	5.10 (2.19)	−1.55
		0.6	3.99 (0.34)	−1.99	8.98 (2.12)	−1.92	9.34 (1.40)	−1.59
	MT-HS, MC-HS	0.1	3.24 (0.56)	−1.69 (0.40)	5.50 (2.59)	−2.15 (0.20)	7.12 (3.52)	−3.07 (0.21)
	Cyclic	0.1	3.37 (0.42)	−1.58 (0.07)	6.19 (2.24)	−0.44 (0.18)	9.24 (2.54)	−1.18 (0.14)
		0.3	3.79 (0.35)	−1.62 (0.06)	8.97 (1.14)	−0.35 (0.17)	11.6 (2.10)	−1.16 (0.15)
Mortar Cubes forCS	MT, MC	0	1.95 (0.10)	−1.90 (0.02)	11.64 (1.94)	−2.02 (0.18)	19.0 (1.30)	−2.72 (0.23)
	Cyclic	0	2.08 (0.23)	−1.78 (0.13)	1.83 (2.75)	−2.66 (0.60)	12.47 (5.23)	−3.57 (0.51)
Mortar Cubes for CB	MT, MC	0	1.54 (0.04)	−1.82 (0.06)	2.43 (0.59)	−3.10 (0.32)	5.38 (2.06)	−3.85 (0.33)
	Cyclic	0	1.49 (0.15)	−1.91 (0.07)	2.14 (0.43)	−3.62 (0.59)	3.98 (0.99)	−4.25 (0.42)

Note: Pre-C Level = Pre-compression Level; Comp = Compressive.

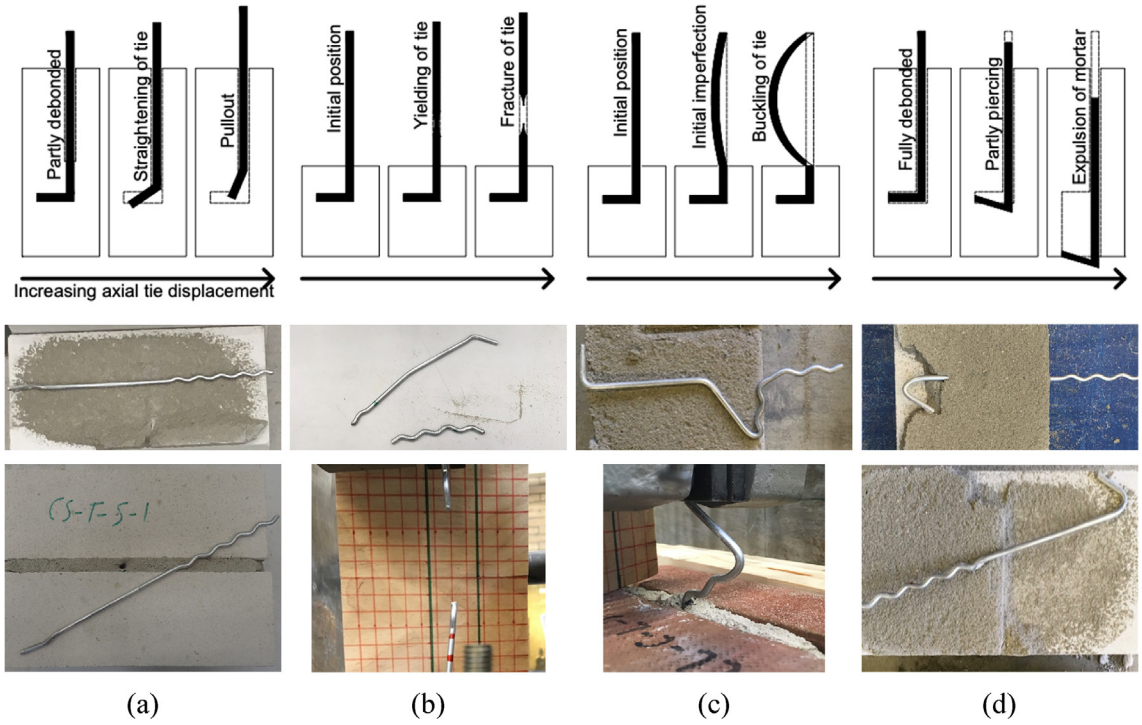

Fig. 4. Failure mode sequence: Type A (a), Type B (b), Type C (c) and Type D (d).

is the most common failure mode in tension, and only a few connections failed due to the tie failure. 92% of the specimens was failed in the sliding failure (Type A). In the former case failure occurs due to poor bonding between the tie and the mortar and due to the low strength of the mortar. In the latter case, the mortar and the couplet remain intact, thus neither cracks in the mortar joints nor detachment at the brick–mortar interface are observed.

Regarding the compressive loading, the couplets showed either of the two failure mechanisms:

- Buckling failure (Type C): the failure is caused by buckling of the tie (Fig. 4c)
- Expulsion failure (Type D): the failure is achieved by piercing and expulsion of the cone of mortar around the tie (Fig. 4d)

The large majority of the couplets loaded in compression was characterized exhibiting buckling failure. Only in 8% of the tested couplets the expulsion failure was observed. It should be noted that the description of the evolution of the failure mechanisms, as presented in Fig. 4, was obtained by stopping a number of additional tests apart from the main specimens at different values of the imposed displacement and, when needed, the test was stopped for opening the specimens by performing bond wrench tests to observe the condition of the tie embedded in the mortar. The results of the additional tests were used to investigate the evolution of the failure mechanism and to define the flexural strength of the couplets via the bond wrench tests.

Fig. 5 shows the force–displacement curves for CS-70 couplets for monotonic loading. It should be noted that the whole curves are reported beyond the point of failure. The figure shows also the average curve obtained by averaging the data from eleven specimens as an example. The average curves of each testing group are presented in Fig. 6. In CS-70 specimens, three different failure modes were observed: Type A (100%) for monotonic tensile loading, and Type C (82%) or Type D (18%) for compressive loading. Regarding the monotonic tensile loading, the peak strength was reached when the hooked part of the tie started straightening, followed by the sliding between the mortar and the tie. An initial linear elastic behavior of the connection up to about half of the peak load was followed by hardening up to the peak. The post-peak phase was characterized by gradual softening up to large displacements (50 mm). A qualitatively similar behavior was obtained irrespectively on the applied pre-compression level and loading rate.

In compression, the linear-elastic behavior of the connection was observed up to the peak load, that was achieved due to either buckling of the tie, or expulsion of the cone of mortar. A drastic reduction of resistance was observed in the post-peak phase. The behavior of the specimens was consistent for every test regardless of the failure modes.

As regards the cyclic tests on CS-70 specimens, an example full cyclic curve which is characterized by pinching effect as well as its envelope curve is presented in Fig. 7. The results of the cyclic tests are given in terms of envelope curves in Fig. 8.

As shown in Fig. 8, nonlinear force–deformation response was detected even in the initial loading stages. After the peak load was reached, a pronounced pinching effect was observed. This behavior primarily occurred due to the loss of bond strength around the tie-mortar interface and crushing of the mortar around the hook. The backbone curves were similar to those obtained for the monotonic tests, and the failure mode of the specimens was a combination of the mechanisms described for the monotonic tests. When the failure mode was a combination of Type A and Type C, at the end of the test the tie failed with rupture due to deterioration of mortar. The peak load in tension obtained for cyclic loading was lower than that obtained during the corresponding monotonic tests and the post-peak behavior was more brittle.

CS-70-15D specimens are characterized by the embedment of the hooked end of the tie in CS couplets with an embedment length of 70 mm and 15-degree bent tie. Bent ties were studied to represent the real case installation situation from the field, as seen in common construction practice. Fig. 9 illustrates the force–displacement curves obtained for monotonic loading by averaging

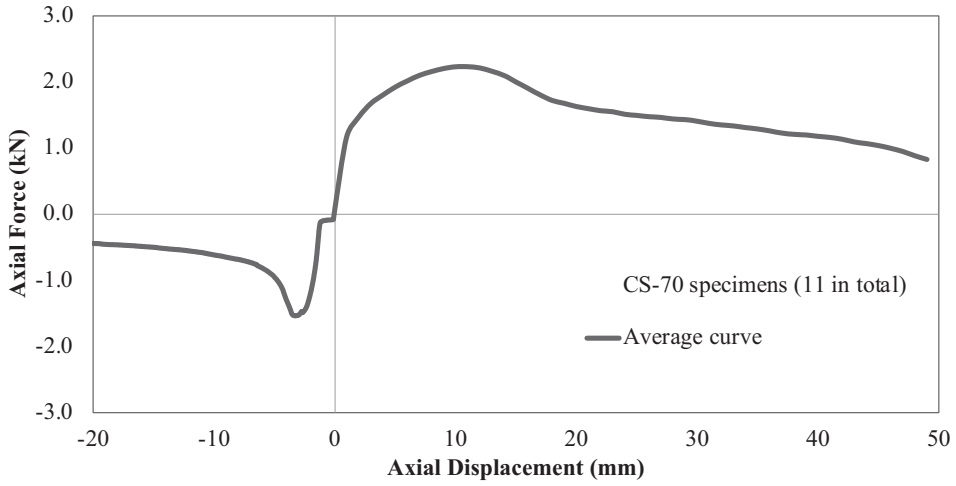

Fig. 5. Experimental results of CS specimens with 70 mm anchored length for a pre-compression level of 0.1 MPa.

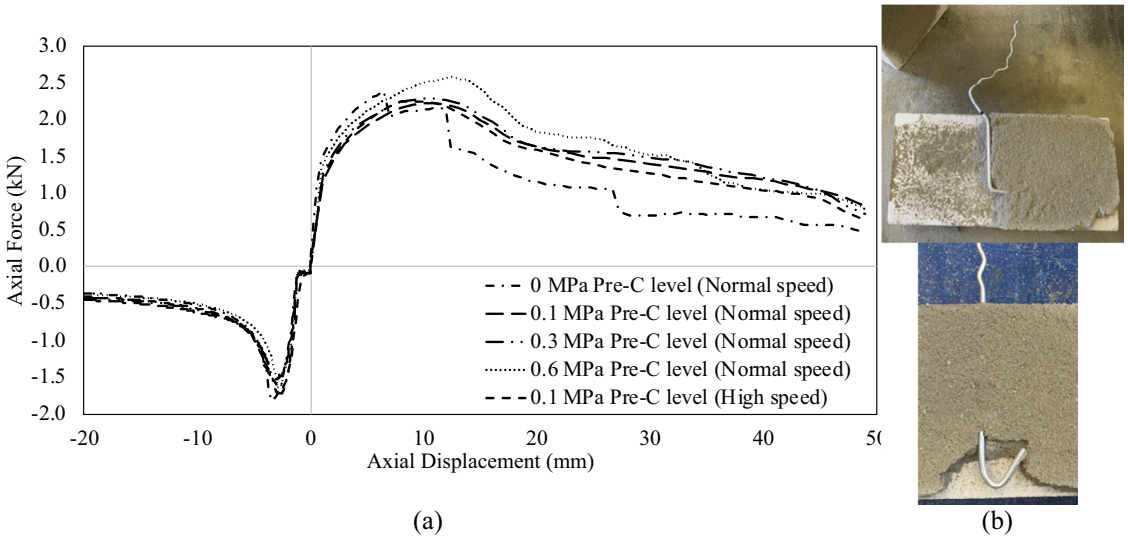

Fig. 6. Average results for monotonic loading for CS specimens with 70 mm anchored length (a) and observed failure mechanisms (b).

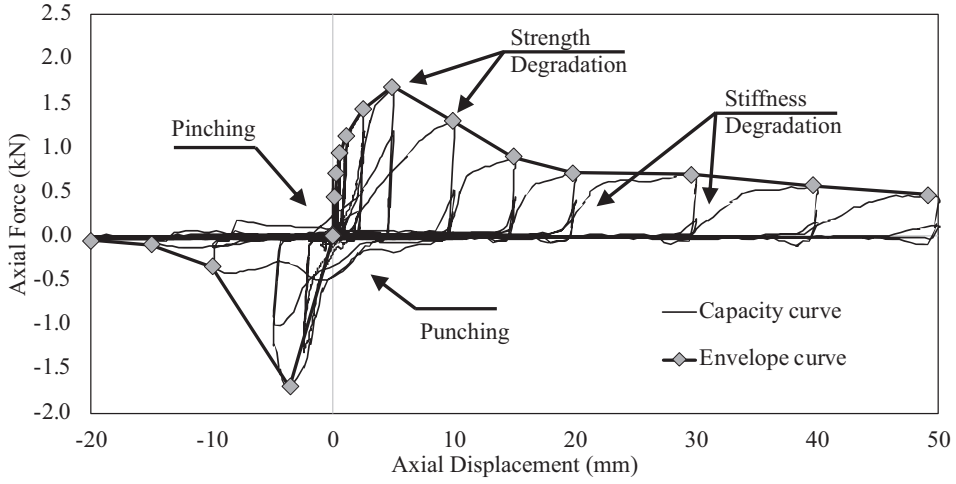

Fig. 7. Force-displacement envelope curve for CS specimens with 70 mm anchored length.

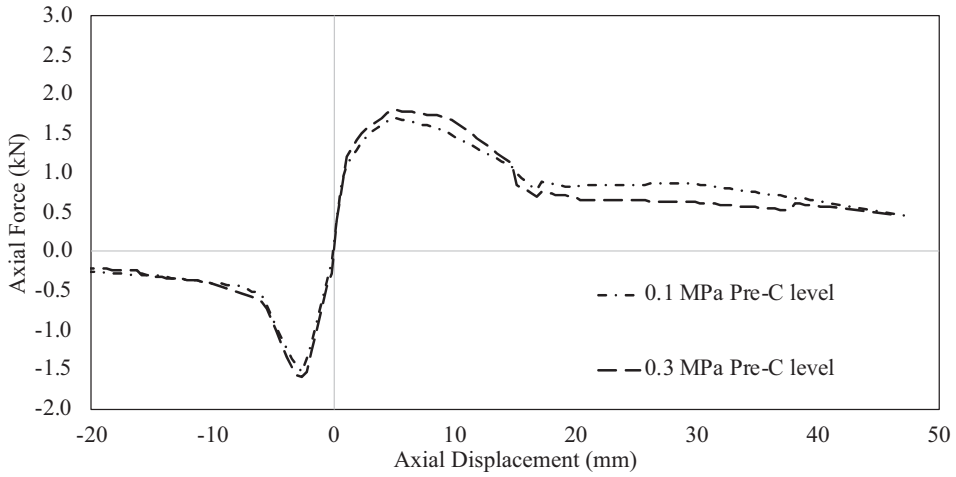

Fig. 8. Summary of results for cyclic loading for CS specimens with 70 mm anchored length.

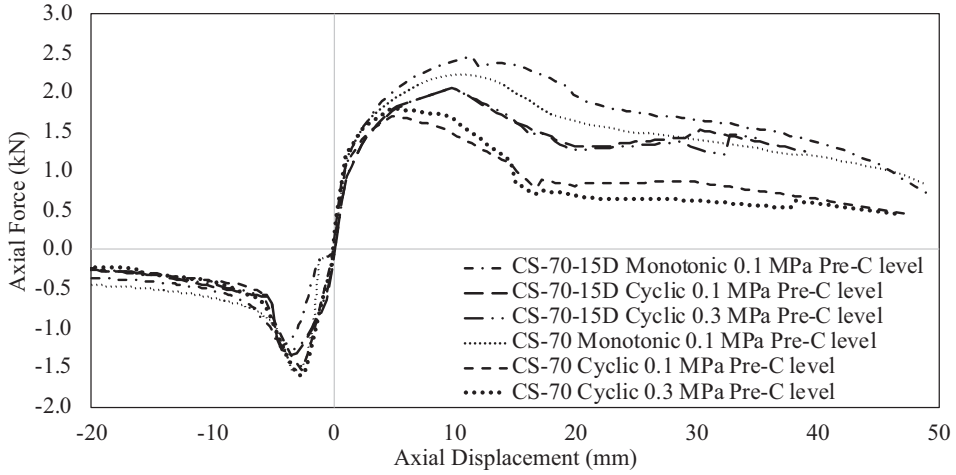

Fig. 9. Summary of results for monotonic and cyclic loading for bent and non-bent tie for CS specimens with 70 mm anchored length.

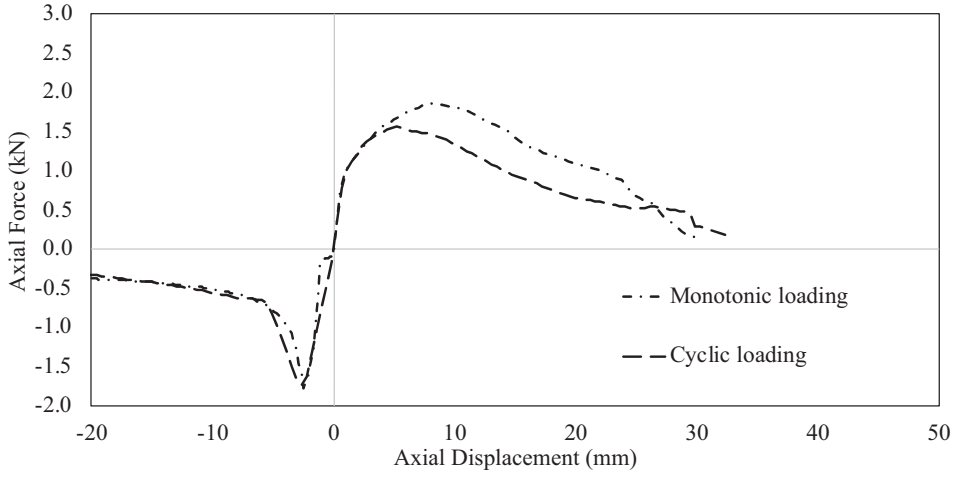

Fig. 10. Summary of results for monotonic and cyclic loading for CS specimens with 50 mm anchored length.

the single force–displacement data at a pre-compression level of 0.1 MPa and the average envelope curves for cyclic loading for different lateral pre-compression levels. The observed failure mechanisms were Type A (100%) and Type C (100%) for monotonic tensile and compressive loading, respectively, and a combination of these two mechanisms for the cyclic tests. The curves for monotonic and cyclic loading were very close to each other in the initial loading and diverge when the displacement increased; however, the curves

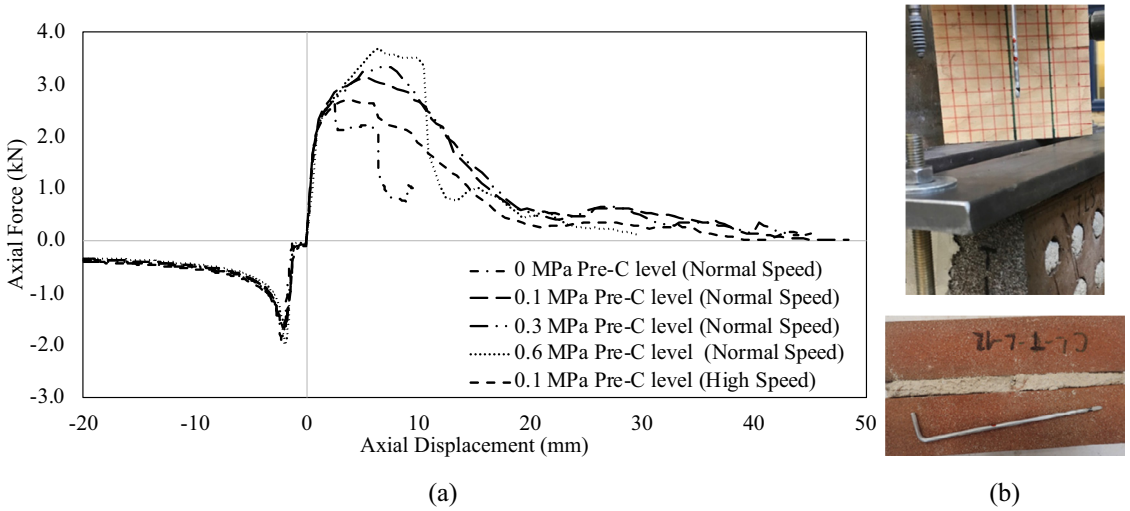

Fig. 11. Summary of results for monotonic loading for CB specimens (a) and observed failure mechanisms (b).

for cyclic loading at pre-compression levels of 0.1 MPa and 0.3 MPa were very close to one another during all loading. In tension, the force–displacement curve is linear up to about one-third of the peak load, and then characterized by a hardening branch. In compression, nonlinear behavior was observed even in the initial loading stage. The envelope curves for cyclic loading were characterized by smaller force values for tensile displacements, while the peak compressive force was slightly larger for cyclic tests.

CS-50 specimens are characterized by an embedment length of the hooked end of the tie in CS couplets equal to 50 mm. Fig. 10 shows the average force–displacement curves obtained for monotonic loading, as well as the average envelope curves for cyclic loading, both monotonic and cyclic tests performed at a pre-compression level of 0.1 MPa. The failure behavior of the corresponding specimens under tensile loading was defined by Type A, while under compressive loading, it was defined by Type C. The characteristic behavior of the connection was similar with CS specimens with 70 mm anchored length: straightening of the tie under tension and buckling under compressive loading. The force–displacement curve in tension stage was found to be linear up to about one-half of the peak load after which the behavior was detected nonlinear, while regarding the compressive stage, it was found that a straight portion of the force–displacement curve was up to the peak load. The failure mode of the specimens regarding the cyclic tests was a combination of the mechanisms described for the monotonic tests.

CB-50 specimens are characterized by the embedment of the zigzagged end of the tie in CB couplets with an embedment length of 50 mm. The following variations were performed for CB-50 specimens for the monotonic tests: four different pre-compression levels and two different rate of load application, as shown in Fig.11. Fig. 12 shows the force–displacement average curves obtained for each corresponding variation. Two types of failure mode were observed regarding the monotonic tensile loading: Type A and Type B; while for the monotonic compressive loading, the failure mode was Type C. Regarding the monotonic tensile loading, the peak of resistance of the specimens was achieved either when the tie reached the ultimate capacity of the tensile strength of 4.1 kN or when the bed joint started crushing of the surrounding mortar and tie. The position of fracture was observed next to the embedment of the tie due to geometry of the tie, and at the end of the test the tie failed with brittle rupture. The force–displacement curve started with a linear part up to about

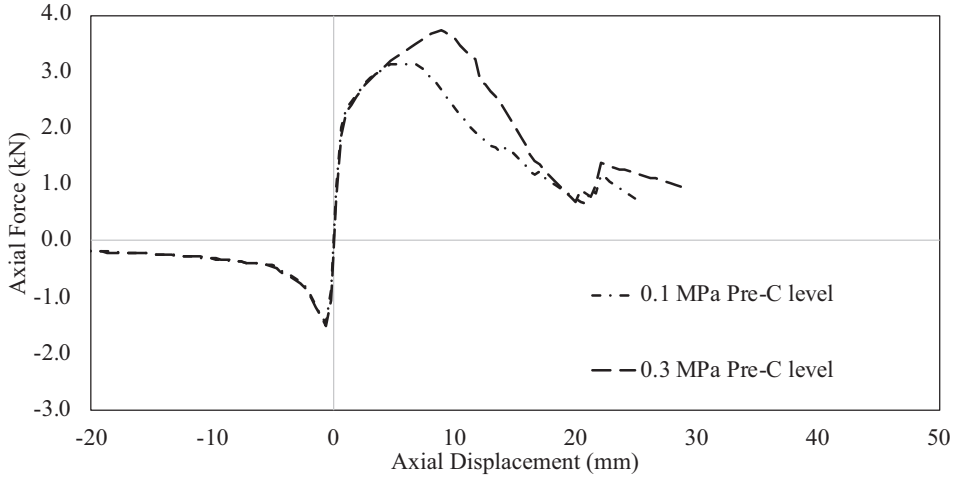

Fig. 12. Summary of results for cyclic loading for CB specimens in terms of envelope curves.

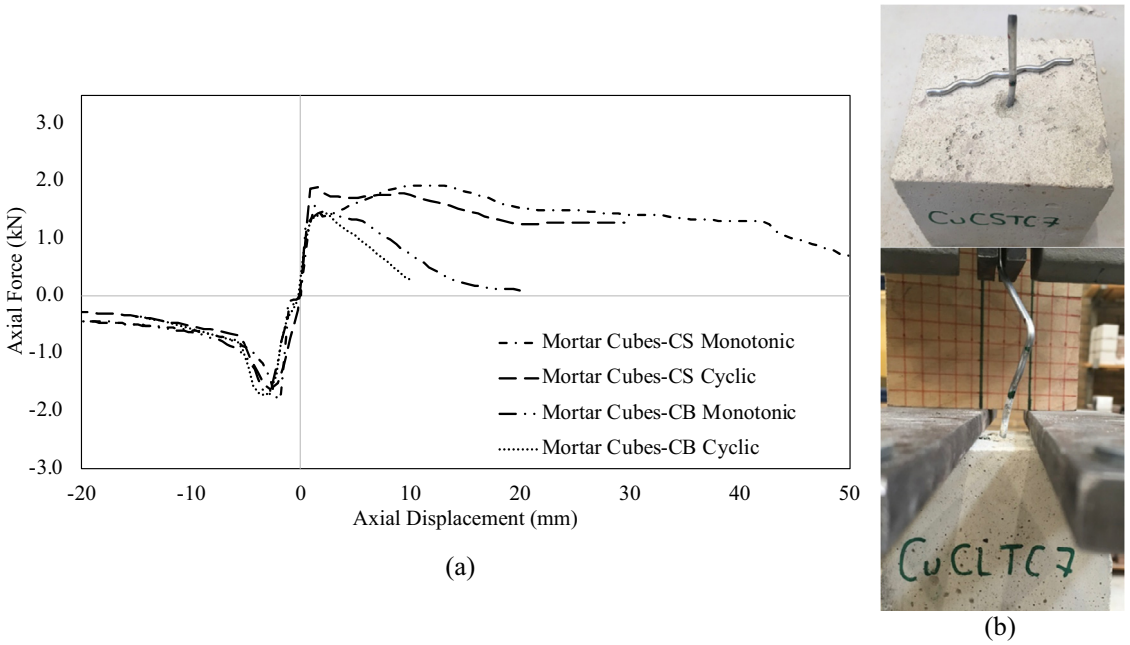

Fig. 13. Summary of results for CS and CB mortar cubes (a) and observed failure mechanism (b).

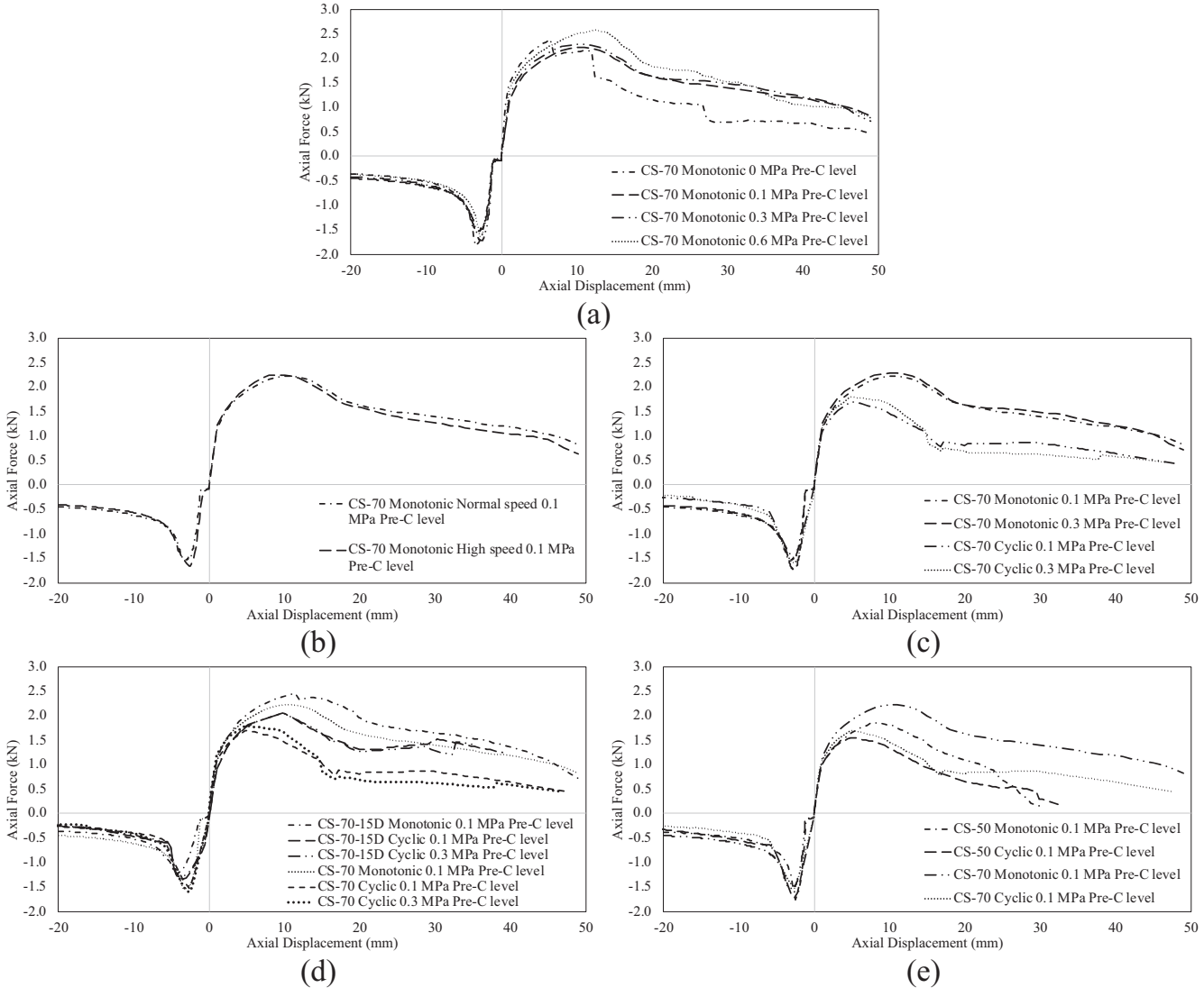

Fig. 14. Force-displacement curve comparison of variations for CS specimens.

one-half of the peak load. After that point hardening took place up to the peak load. Both failure modes showed a rather brittle post-peak behavior.

For the monotonic compressive loading, the peak of resistance of the specimens, independently of the applied pre-compression level and speed rate, was achieved when the tie buckled. Compressive behavior started with a linear portion up until the compressive strength was reached. A hyperbolic reduction of resistance was detected in the post-peak phase. The behavior of the specimens was consistent for every test.

Fig. 12 shows the average envelope curves of the CB-50 specimens for the cyclic loading. For these specimens, only two pre-compression levels (0.1 MPa and 0.3 MPa) were investigated. The behavior and the failure mode of the specimens under cyclic loading was a combination of those observed for the monotonic tensile and compressive loading. Additionally, it was observed that the cyclic behavior was nonlinear and asymmetry since the early loading stage, and, after the peak load was reached, the force–displacement curves were characterized by the pinching effect for increasing displacements.

The ties embedded inside CS and CB mortar cubes were tested under monotonic and cyclic loading in order to decouple the mortar-tie interaction from other possible influencing parameters. Fig. 13 shows the average force–displacement curves for both monotonic and cyclic loading (in the latter case the envelope curves) of ties embedded in CS and CB mortar cubes. When the cubes were subjected to monotonic tensile loading, the failure mechanism was the same observed for the ties embedded in couplets: crushing of the mortar and straightening of the tie (Type A). During the loading history, a first peak was achieved when the bond strength capacity was reached between tie and mortar. The peak of resistance of the specimens was then attained after straightening of the tie. After peak, the observed reduction of capacity was rather ductile for the CS mortar cubes, and more brittle for the CB mortar cubes. In compression only buckling of the tie (Type C failure) was observed for both CS and CB mortar cubes. A qualitatively similar behavior was obtained for each specimen, with a hyperbolic reduction of the resistance in the post-peak phase. The observed failure mode of cubes for the cyclic loading was a combined failure mode of monotonic loading.

To have a detailed understanding of the obtained results the average force-displacements curves defined for every testing variation of the CS specimen are shown in Fig. 14. The test has been performed with different type of variations: two embedment lengths, four pre-compression levels, two different tie geometries, and five different testing protocol for CS specimens. It was observed that the levels of pre-compression had negligible influence on the behavior of connections (Fig. 14a). Similarly, the loading rate had also no influence on the behavior (Fig. 14b). On the contrary the loading repetition led to a significant decrease of the specimens' strength, even though stiffness and ductility did not change (Fig. 14c). When bent ties are considered (Fig. 14d), an increase of capacity in tension was observed and vice versa in compression.

In a similar way, also the CB specimens were tested under different conditions: four different pre-compression levels, and five different testing protocol. For CB specimens, it can be observed that the peak strength increases with the lateral pre-compression (Fig. 15a), highlighting the presence of dowel effect on the specimen behavior. On the other hand, neither the loading repetition (Fig. 15b) nor the loading rate (Fig. 15c) affects significantly the results.

Regarding the tests of specimens with mortar cubes, the behavior of the ties embedded in CS mortar is similar to that observed when the ties are embedded in the couplets (Fig. 16a), while the force capacity of the ties with CB mortar is halved when they are embedded in the mortar cubes (Fig. 16b) due to absence of dowel effect. Note that, the numerous small hollows present in the perforated CB specimens provide extra resistance due to a dowel effect.

Comparing the results obtained during a previous campaign also performed at the laboratory of TU Delft [20] and those presented in this paper, the significantly higher resistance observed

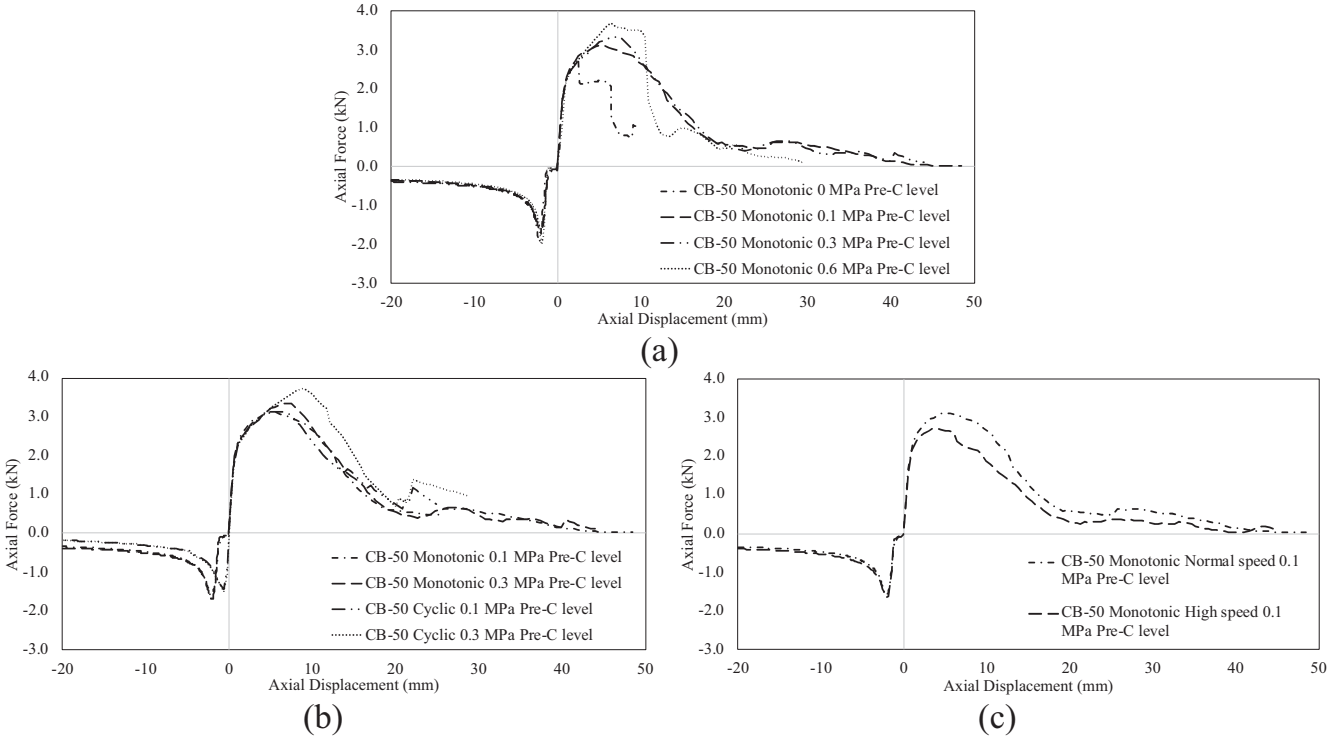

Fig. 15. Force-displacement curve comparison of variations for CB specimens.

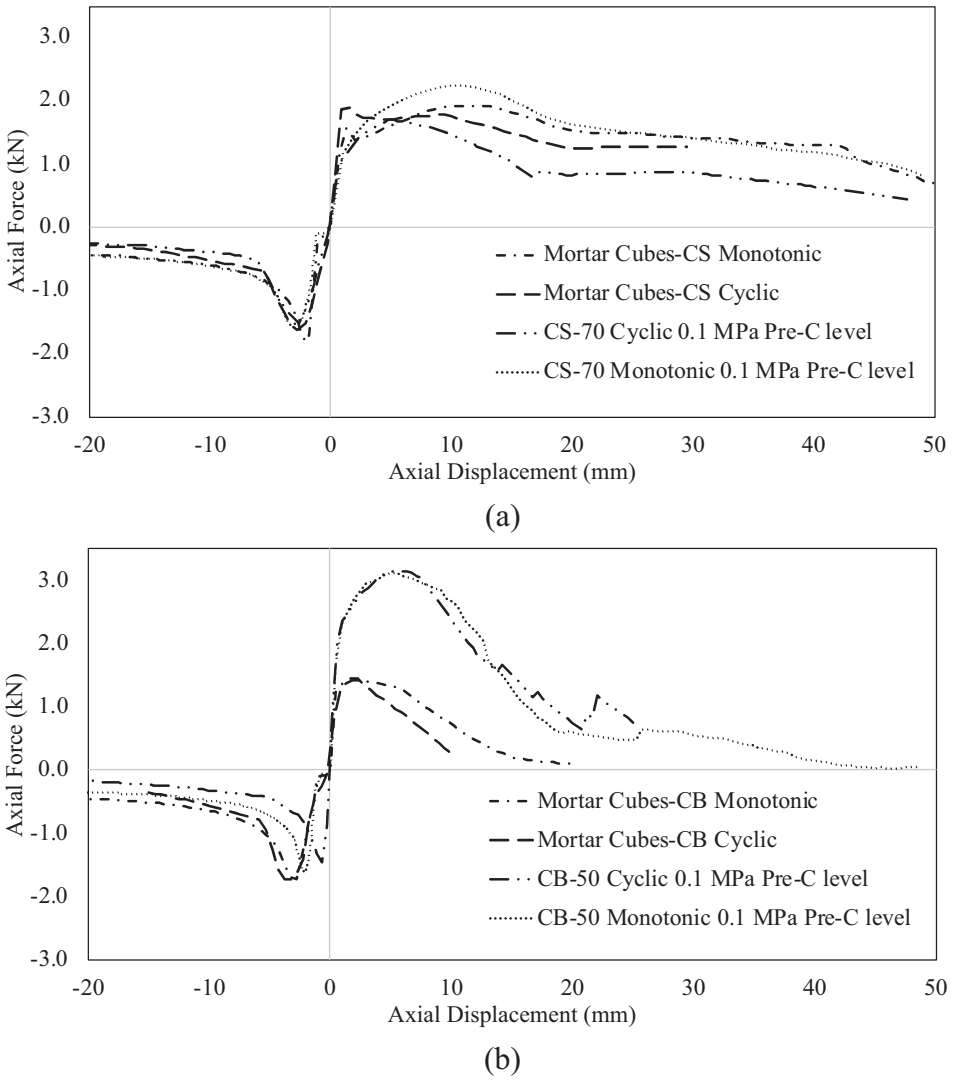

Fig. 16. Force-displacement curve comparison of variations for CS (a) and CB (b) mortar cubes.

in the current campaign is probably caused by an improved quality of the specimens and better workmanship. Namely, thanks to higher precision and consistency during the construction phase, the specimens have developed higher mechanical properties. Considering the current campaign, very consistent results were obtained, while during previous experimental campaigns, the bond between the tie and the mortar of a number of specimens failed in a very early loading stage due to the poor mechanical properties.

4. Conclusions

This paper aims at assessing the seismic response of the wall metal tie connections in typical Dutch masonry double-leaf cavity walls which are composed of an inner load-bearing leaf made of calcium silicate brick masonry and an outer leaf made of clay brick masonry. The tie was pulled from either a calcium silicate (CS) couplet or a clay brick (CB) couplet. This section discusses and compares the experimental results obtained under monotonic tensile and compressive loading, as well as cyclic loading, and for different connection geometry and loading protocols.

The following results are reported:

- Comparing the experimental results of the monotonic and cyclic tests in terms of the peak load, on average a 19% larger peak load is observed for monotonic tests for the CS specimens, and a similar increase in peak load is observed also for the CB specimens.
- Larger values of the bond strength are obtained for the CB couplets thanks to dowel action of the mortar in the brick holes. For the same reason, a significant reduction of pull-out strength is obtained when the ties are embedded in the mortar cubes compared to the couplets.
- Overall, it can be concluded that the behavior of the studied wall-tie connection is mainly governed by the behavior of tie embedment in the CS leaf.

The studies carried out in this experimental campaign may improve the knowledge of the connection between the leaves in cavity walls which can be helpful to identify and validate suitable assessment methods and retrofit interventions. The findings of this study can help improving the testing, standardization and eventually design of the wall-to-wall metal ties, which the construction

industry benefits from in the long run. As a finding of such, it can be suggested that the bonding between the tie and the mortar, and the tie stiffness can be improved for the companies for new products. Taking a wider outlook, the experimental campaign have clarified some aspects of the behavior of cavity wall ties under axial loading; however further research can be conducted to fully understand the characteristic of the cavity wall ties. Hence, solid clay bricks for the load-bearing wall, same mortar for both of the cavity leaves and corrugated metal wall ties can be investigated. Additionally, the interaction with shear loading should be studied.

5. Data availability statement

The experimental data are available in a public repository online in accordance with funder data retention policies. The dataset consists of measured force–displacement cyclic responses of all the specimens exhibited in this paper. Proper referencing to the repository file, with its DOI number, has been made in the paper when relevant.

CRediT authorship contribution statement

Onur Arslan: Writing - original draft. **Francesco Messali:** Supervision, Writing - review & editing. **Eleni Smyrou:** Supervision, Writing - review & editing. **İhsan Engin Bal:** Supervision, Writing - review & editing. **Jan Gerrit Rots:** Supervision, Writing - review & editing.

Declaration of Competing Interest

The authors declare that they have no known competing financial interests or personal relationships that could have appeared to influence the work reported in this paper.

References

[1] NEN-EN (Nederlands Normalisatie-instituut) (2016). "Specification for ancillary components for masonry - Part 1: Wall ties, tension straps, hangers and brackets.". NEN-EN 845-1.
[2] F. Messali, R. Esposito, S. Jafari, G.J.P. Ravenshorst, P.A. Korswagen Eguren, J.G. Rots (2018). "A multiscale experimental characterisation of Dutch unreinforced masonry buildings." Proc., 16th European Conference on Earthquake Engineering (ECEE), Thessaloniki, Greece.
[3] R. Esposito, K.C. Terwel, G.J.P. Ravenshorst, H.R. Schipper, F. Messali, J.G. Rots (2017). "Cyclic pushover test on an unreinforced masonry structure resembling a typical Dutch terraced house." Proc., 16th World Conference on Earthquake, Santiago, Chile.
[4] R. Esposito, F. Messali, G.J.P. Ravenshorst, H.R. Schipper, J.G. Rots, Seismic assessment of a lab-tested two-storey unreinforced masonry Dutch terraced house, Bul. Earthq. Eng. 17 (8) (2019) 4601–4623.
[5] F. Graziotti, A. Penna, G. Magenes, A comprehensive in situ and laboratory testing programme supporting seismic risk analysis of URM buildings subjected to induced earthquakes, Bull. Earthq. Eng. 17 (8) (2019) 4575–4599.
[6] F. Graziotti, U. Tomassetti, S. Kallioras, A. Penna, G. Magenes, Shaking table test on a full scale URM cavity wall building, Bull. Earthq. Eng. 15 (12) (2017) 5329–5364.
[7] U. Tomassetti, A.A. Correia, P.X. Candeias, F. Graziotti, A. Campos Costa, Two-way bending out-of-plane collapse of a full-scale URM building tested on a shake table, Bull. Earthq. Eng. 17 (4) (2019) 2165–2198.
[8] F. Graziotti, U. Tomassetti, A. Penna, G. Magenes, Out-of-plane shaking table tests on URM single leaf and cavity walls, Eng. Struct. 125 (2016) 455–470.
[9] F. Graziotti, U. Tomassetti, S. Sharma, L. Grottoli, G. Magenes, Experimental response of URM single leaf and cavity walls in out-of-plane two-way bending generated by seismic excitation, Constr. Build. Mater. 195 (2019) 650–670.
[10] K.Q. Walsh, D.Y. Dizhur, J. Shafaei, H. Derakhshan, J.M. Ingham, In situ out-of-plane testing of unreinforced masonry cavity walls in as-built and improved conditions, Structures 3 (2015) 187–199.
[11] D. Reneckis, J.M. LaFave, W.M. Clarke, Out-of-plane performance of masonry veneer walls on wood frames, Eng. Struct. 26 (2004) 1027–1042.
[12] M. Giaretton, D. Dizhur, F. da Porto, J.M. Ingham, Construction details and observed earthquake performance of unreinforced clay brick masonry cavity-walls, Structures 6 (2016) 159–169.
[13] BSI (British Standards Institution). (2010). "Recommendations for the design of masonry structures to BS EN 1996-1-1 and BS EN 1996-2." PD 6697:2010.
[14] H. Derakhshan, W. Lucas, P. Visintin, M.C. Griffith, Out-of-plane Strength of Existing Two-way Spanning Solid and Cavity Unreinforced Masonry Walls, Structures 13 (2018) 88–101.
[15] M. Giaretton, D. Dizhur, J.M. Ingham, Shaking table testing of as-built and retrofitted clay brick URM cavity-walls, Eng. Struct. 125 (2016) 70–79.
[16] H. Derakhshan, W. Lucas, P. Visintin, M.C. Griffith, Laboratory Testing of Strengthened Cavity Unreinforced Masonry Walls, J. Struct. Eng. 144 (3) (2018) 04018005.
[17] Y.-H. Choi, J.M. LaFave, Performance of corrugated metal ties for brick veneer wall systems, J. Mater. Civ. Eng. 16 (3) (2004) 202–211.
[18] D. Reneckis, J.M. LaFave, Seismic Performance of Anchored Brick Veneer (PhD Thesis), Department of Civil and Environmental Engineering, University of Illinois at Urbana-Champaign, 2009.
[19] A. Martins, G. Vasconcelos, A.C. Costa, Experimental assessment of the mechanical behaviour of ties on brick veneers anchored to brick masonry infills, Constr. Build. Mater. 156 (2017) 515–531.
[20] G. Skroumpelou, F. Messali, R. Esposito, J.G. Rots (2018). "Mechanical characterization of wall tie connection in cavity walls." Proc., 10th Australasian Masonry Conference, Sidney, Australia.
[21] NEN-EN (Nederlands Normalisatie-instituut) (1999). "Methods of test for mortar for masonry - Part 3: Determination of consistence of fresh mortar (by flow table)." NEN-EN 1015-3
[22] NEN-EN (Nederlands Normalisatie-instituut) (2012). "Methods of test for ancillary components for masonry - Part 5: Determination of tensile and compressive load capacity and load displacement characteristics of wall ties (couplet test)." NEN-EN 846-5.
[23] ASTM (American Society for Testing and Materials). (2016). "Standard Test Methods for Tension Testing of Metallic Materials." E8 / E8M-16a, West Conshohocken, PA.
[24] ASTM (American Society for Testing and Materials). (2019). "Standard Test Methods of Compression Testing of Metallic Materials at Room Temperature". E9-19, West Conshohocken, PA.
[25] NEN-EN (Nederlands Normalisatie-instituut) (2019). "Methods of test for mortar for masonry - Part 11: Determination of flexural strength of hardened mortar." NEN-EN 1015-11
[26] NEN-EN (Nederlands Normalisatie-instituut) (2005). "Method of test masonry – Part 5: Determination of bond strength by bond wrench method." NEN-EN 1052-5.
[27] FEMA (Federal Emergency Management Agency), (2009). "Quantification of Building Seismic Performance Factors". Document No. FEMA 965, Washington, D.C..
[28] S. Moreira, L.F. Ramos, D.V. Oliveira, P.B. Lourenço, Experimental behavior of masonry wall-to-timber elements connections strengthened with injection anchors, Eng. Struct. 81 (2014) 98–109.
[29] M.N. Fardis (2009). "Seismic Design, Assessment and Retrofitting of Concrete Buildings Based on EN-Eurocode 8". 10.1007/978-1-4020-9842-0.
[30] ASTM (American Society for Testing and Materials). (2019). "Standard Test Methods for Cyclic (Reversed) Load Test for Shear Resistance of Vertical Elements of the Lateral Force Resisting Systems for Buildings." E2126-19, West Conshohocken, PA.
[31] O. Arslan, Supplementary data for the Research on Experimental Characterization of Wall Tie Connections in Cavity Walls, 4TU.Centre for Research Data, Dataset, 2019.